Electronic Supplementary Material (ESI) for Nanoscale.

Plasmon-enhanced fluorescent gold coated novel lipo-polymeric hybrid nanosystem: Synthesis, characterization and application for imaging and photothermal therapy of breast cancer.

Tejaswini Appidi [a†], Rajalakshmi P.S[a†], Shubham A. Chinchulkar[a], Arpan Pradhan[b], Hajira Begum[c], Veeresh Shetty[c], Rohit Srivastava[b] Prabhusankar Ganesan[d] and Dr. Aravind Kumar Rengan [a*]

[a]Dept. of Biomedical Engineering, Indian Institute of Technology Hyderabad, India.

[b]Dept. of Biosciences and Bioengineering, Indian Institute of Technology Bombay, India.

[c]G. Pulla Reddy college of Pharmacy, Hyderabad, India.

[d]Dept. of Chemistry, Indian Institute of Technology Hyderabad, India.

*Corresponding author email: aravind@bme.iith.ac.in

Supporting information

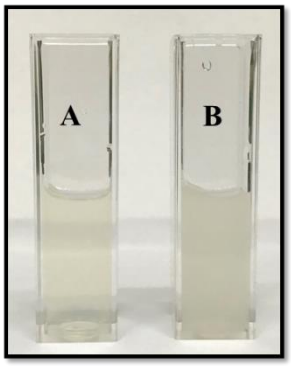

Measurement	A (100 µL of $CaCl_2$)	B (200 µL of $CaCl_2$)
Intensity weighted	188.7±73.59 nm	290.9±138.48 nm
Volume weighted	143.6±56.01 nm	276.3± 131.525
Number weighted	79.6±31.055 nm	85.2 ± 40.54
PDI	0.152	0.227
Zeta potential	-33.56 mV	-41.81 mV

Figure S1: *Synthesis optimization of PDPC NPs. Image showing PDPC NPs formed with A) 100 µL and B) 200 µL of calcium chloride. The tabular column shows the particle size and zeta potential of the particles formed with different concentrations of calcium chloride.*

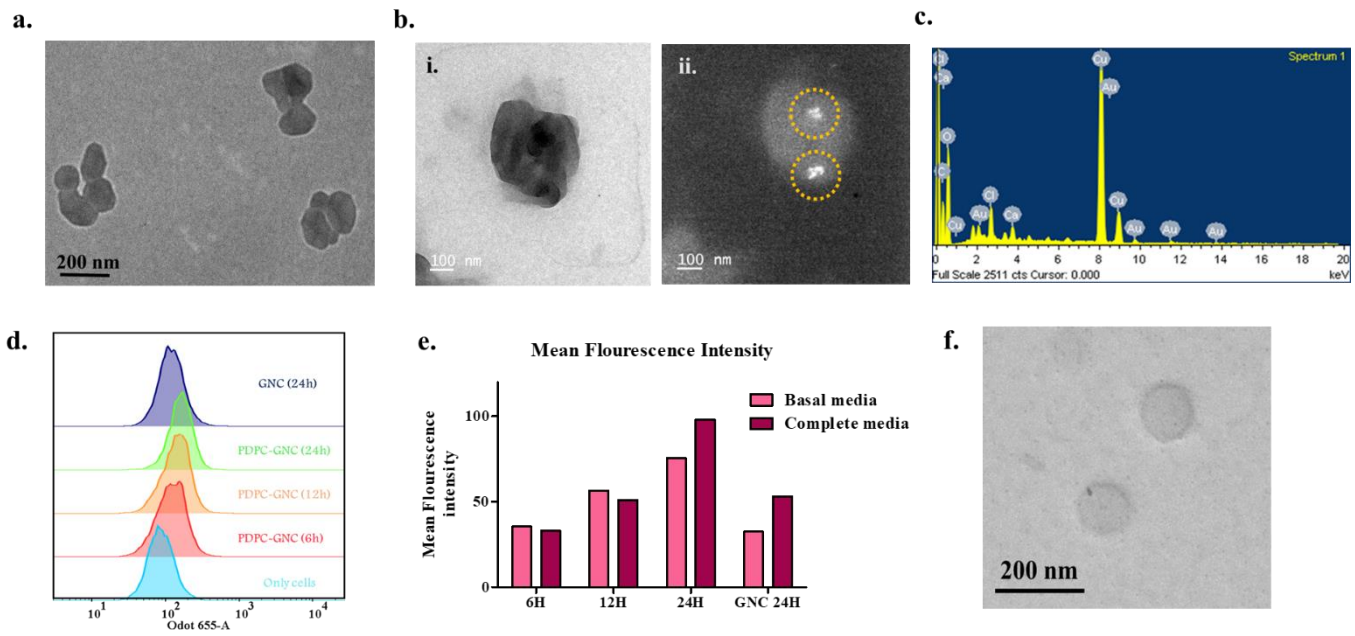

Figure S2: *PDPC-GNC & PDPC-IR NPs. a) TEM image showing PDPC-GNC NPs, b) TEM image of PDPC-GNC NPs in (i) bright and (ii) dark fields (the gold nanoclusters are highlighted in yellow), c) Elemental analysis of PDPC-GNC NPs, d) Cellular uptake of PDPC-GNC NPs in MCF-7 cells incubated with basal media (No FBS), e) Comparison of fluorescence intensity in basal (W/o FBS) and complete media (with FBS) showing the cellular uptake of PDPC-GNC NPs as compared to free GNCs in MCF-7 cells incubated for different time periods, f) TEM image of PDPC-IR NPs.*

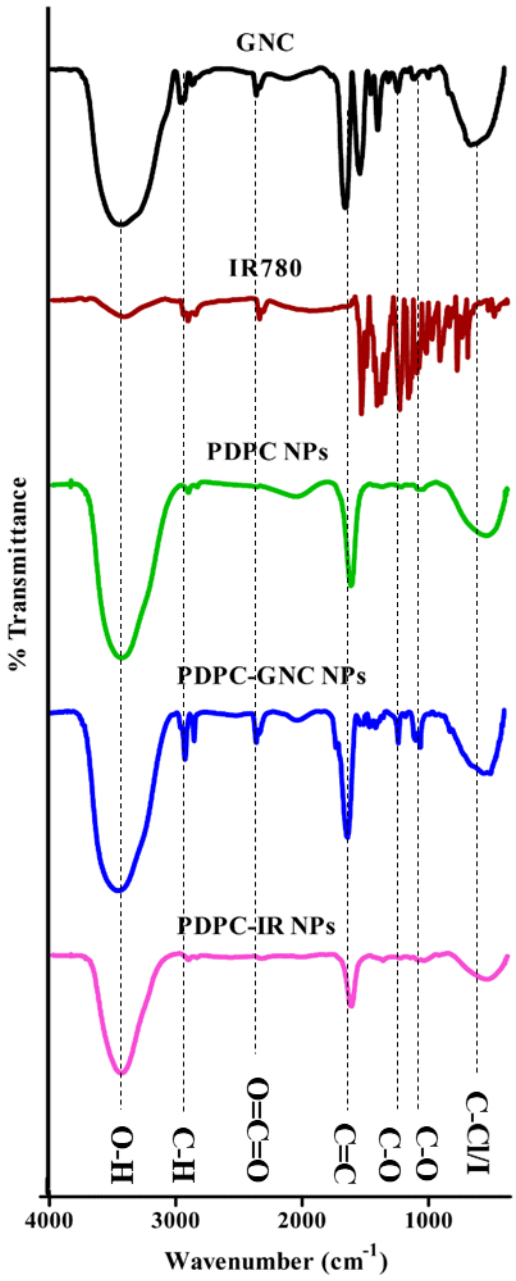

Figure S3*: FTIR analysis of PDPC, PDPC-GNC and PDPC-IR nanoparticles with respective controls.*

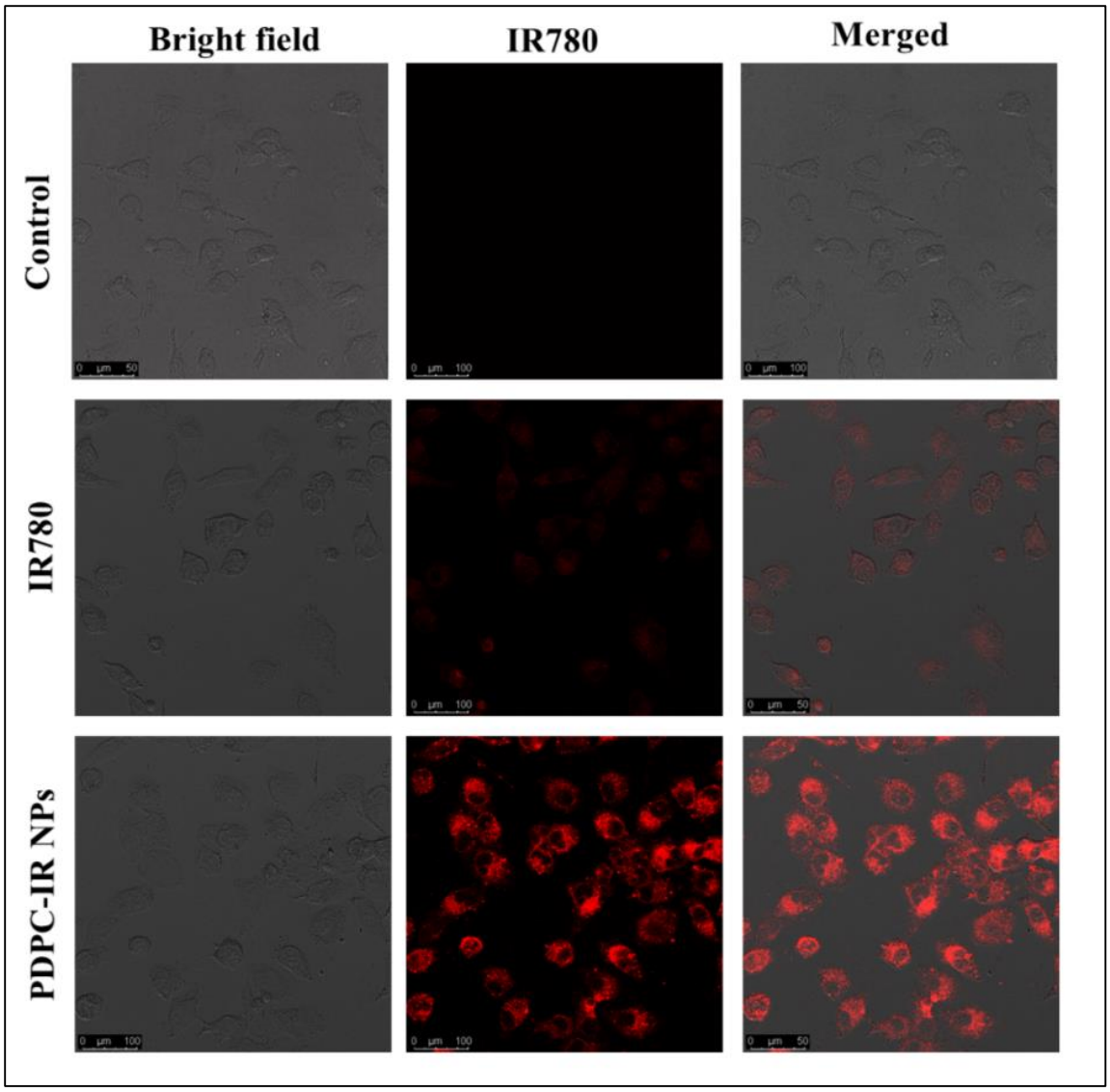

Figure S4: *Cellular uptake of PDPC-IR NPs. Confocal microscopy showing cellular uptake of PDPC-IR NPs in MCF-7 cells (*Scale bar corresponds to 100µm).*

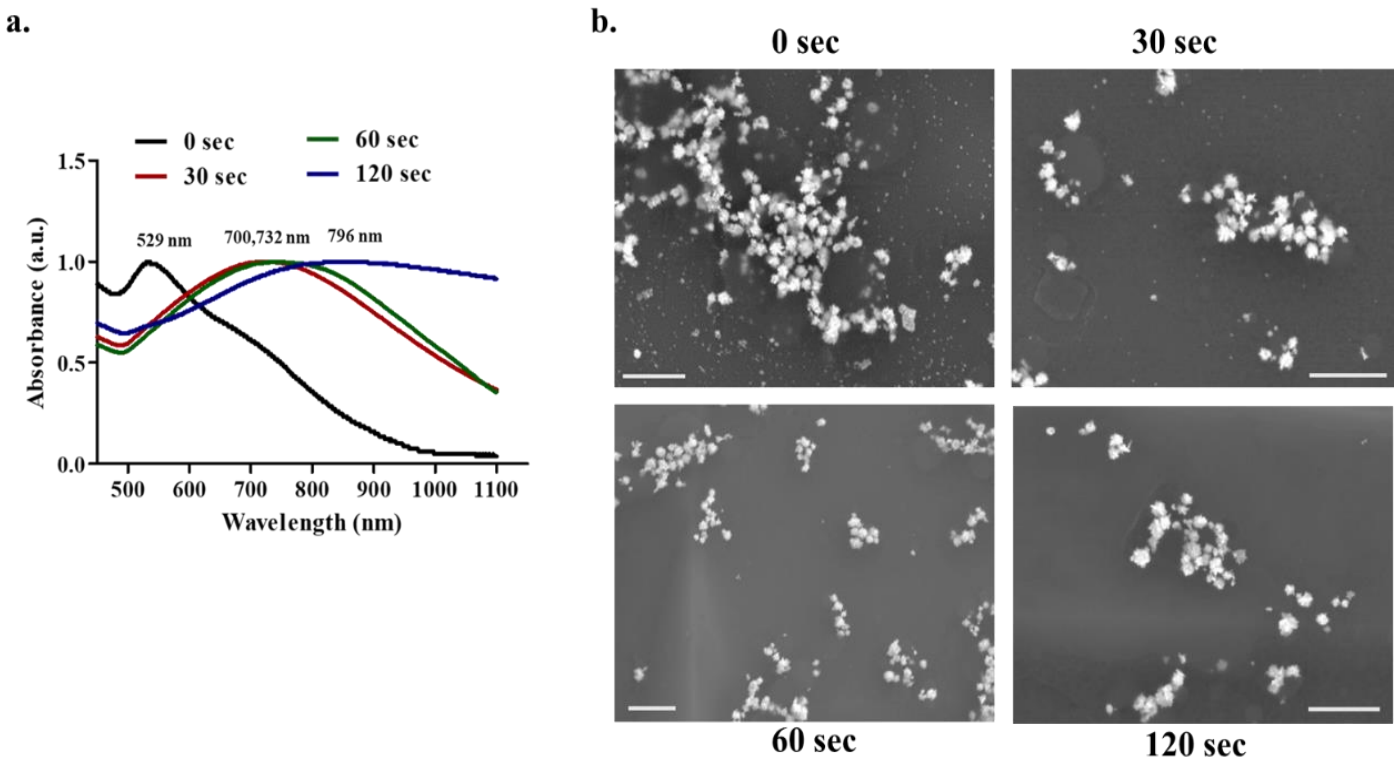

Figure S5: *Formation of PDPC-Au NPs. a) UV-visible absorbance & c) FESEM images at different time points of reaction. (*Scale bar corresponds to 1µm).*

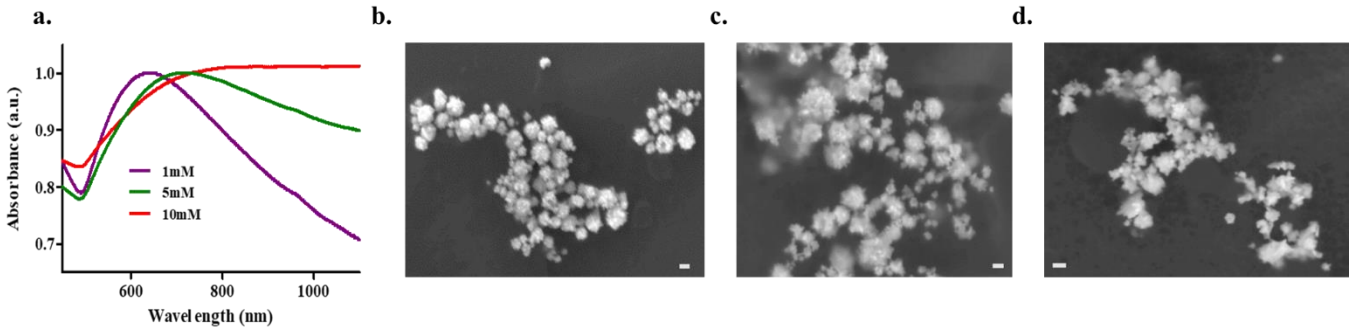

Figure S6: *Optimization of surface coating of PDPC NPs with Au: a) UV-visible spectra of PDPC NPs reacted with different molarities of $HAuCl_4$, FESEM images of PDPC-Au NPs formed with b) 1 mM, c) 5 mM, d) 10 mM $HAuCl_4$ (*Scale bar corresponds to 100 nm)*

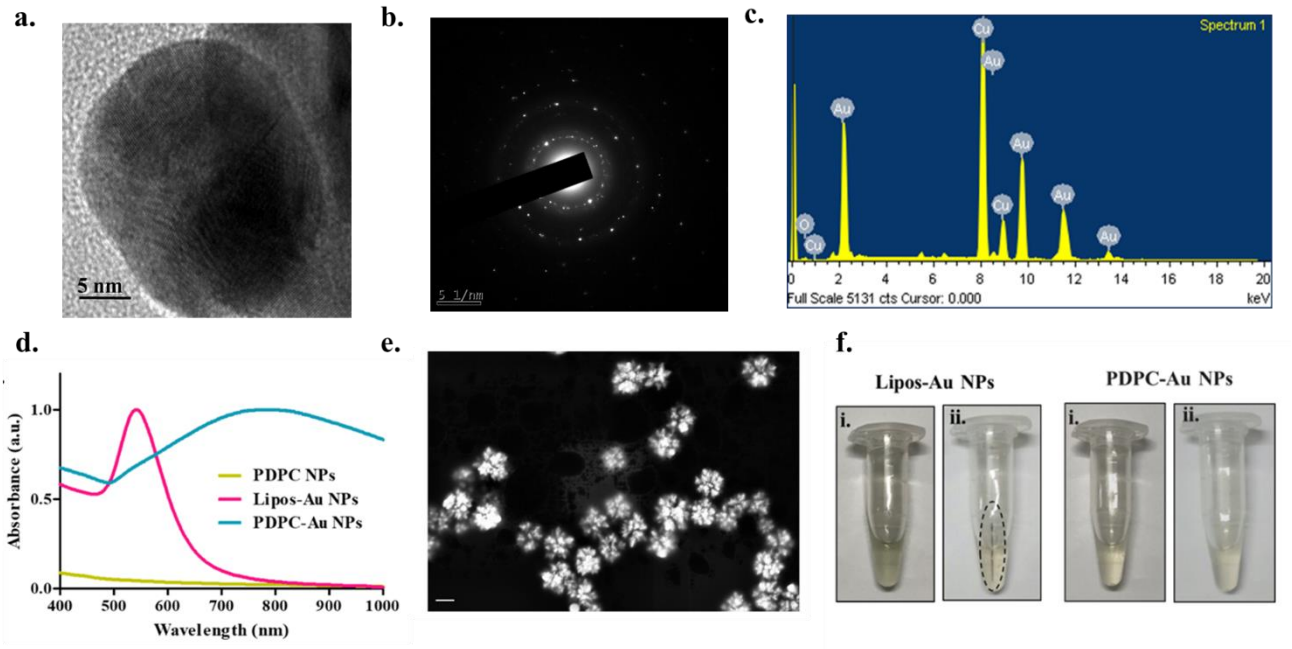

Figure S7: *Characterization of PDPC-Au and Lipos-Au NPs. a) HRTEM image showing the characteristic lattice fringes of Au, b) SAED pattern, c) Elemental analysis of PDPC-Au NPs, d) UV-visible spectra of PDPC, PDPC-Au and Lipos-Au NPs, e) FESEM image of Lipos-Au NPs, f) Stability of PDPC-Au NPs compared to Lipos-Au NPs at i) 0 hours and ii) 36 hours.*

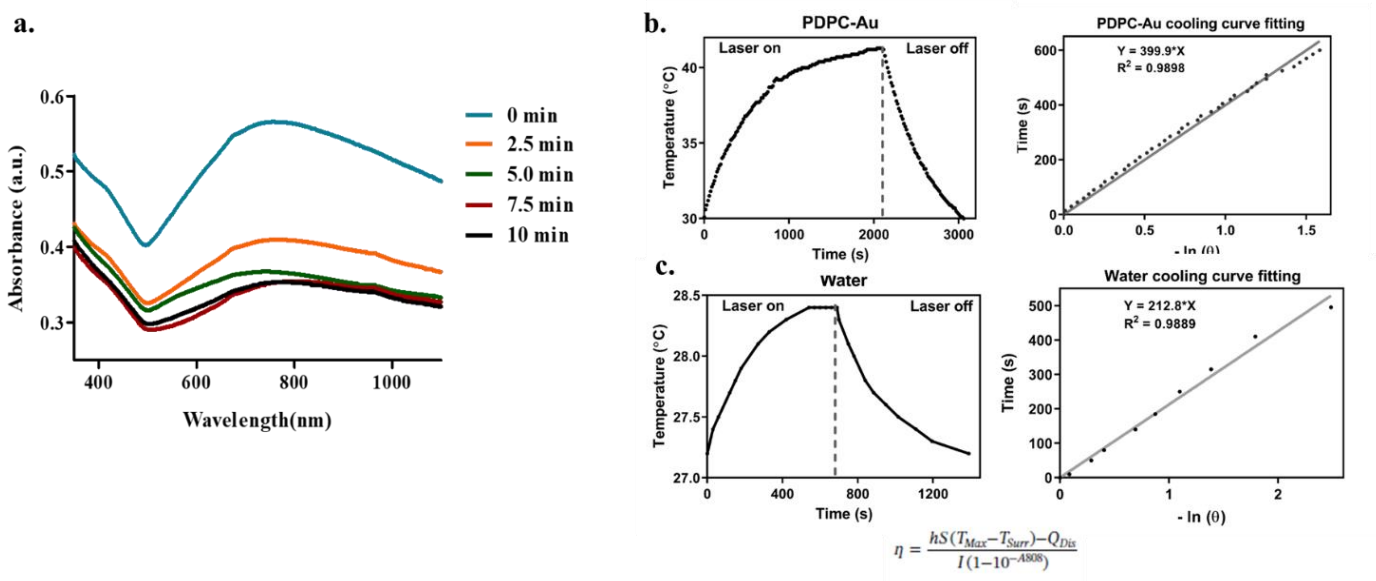

Figure S8: *Photothermal transduction efficacy calculations of PDPC-Au NPs. a) UV-visible spectra showing decrease in NIR (650-900nm) absorbance with laser irradiation, the rise in the temperature and cooling curve fitting for b) PDPC-Au NPs and c) water. The efficacy was calculated to be 65% for PDPC-Au NPs.*

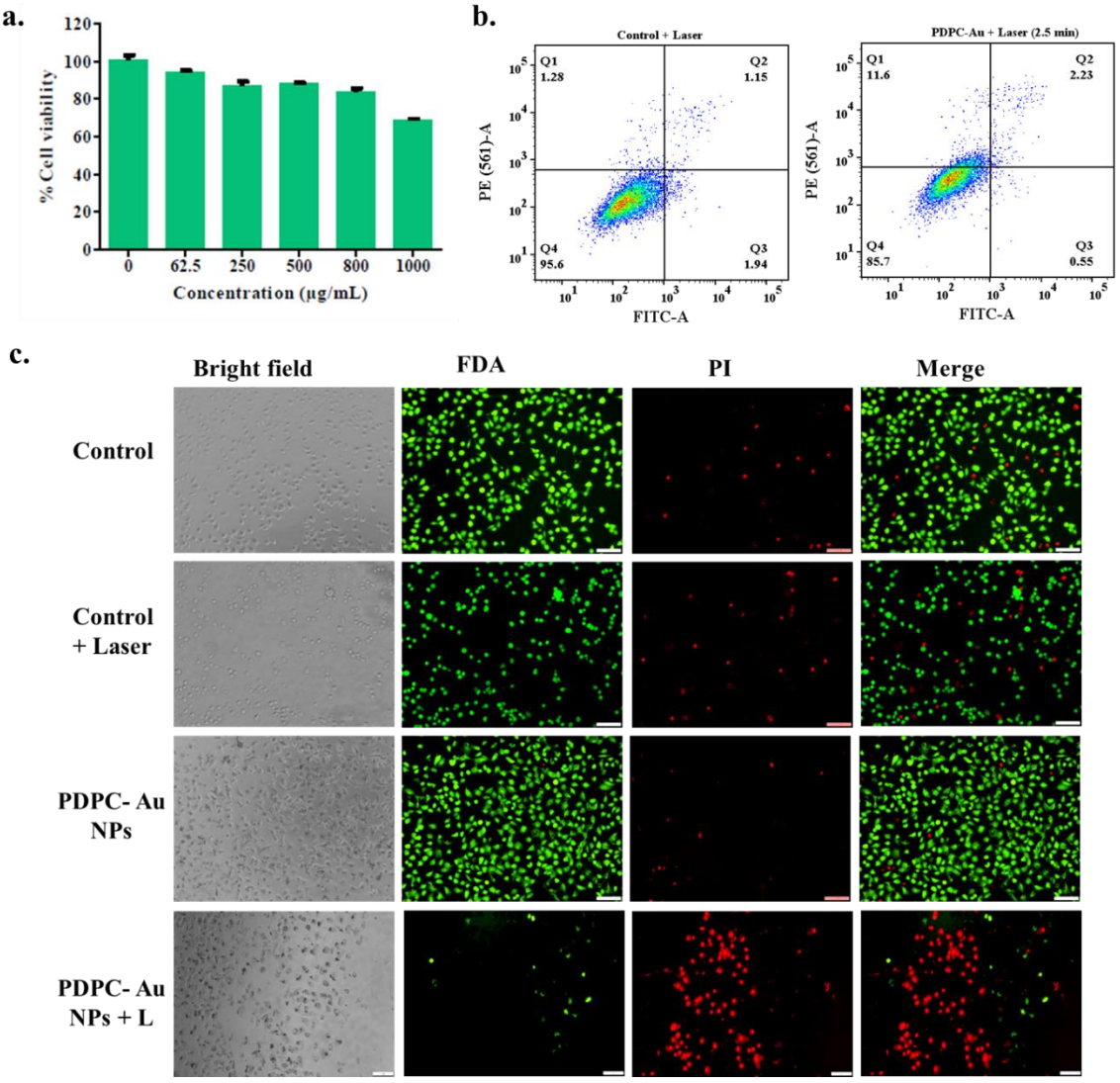

Figure S9: *In-vitro studies of PDPC-Au NPs. a) Biocompatibility of PDPC NPs in L929 cells, b) Annexin V FITC-PI apoptosis studies using PDPC-Au NPs in MCF-7 cells, c) Live/dead assay of PDPC-Au NPs in MCF-7 cells (FDA stains live cells, PI stains dead cells, *Scale bar corresponds to 50µm).*

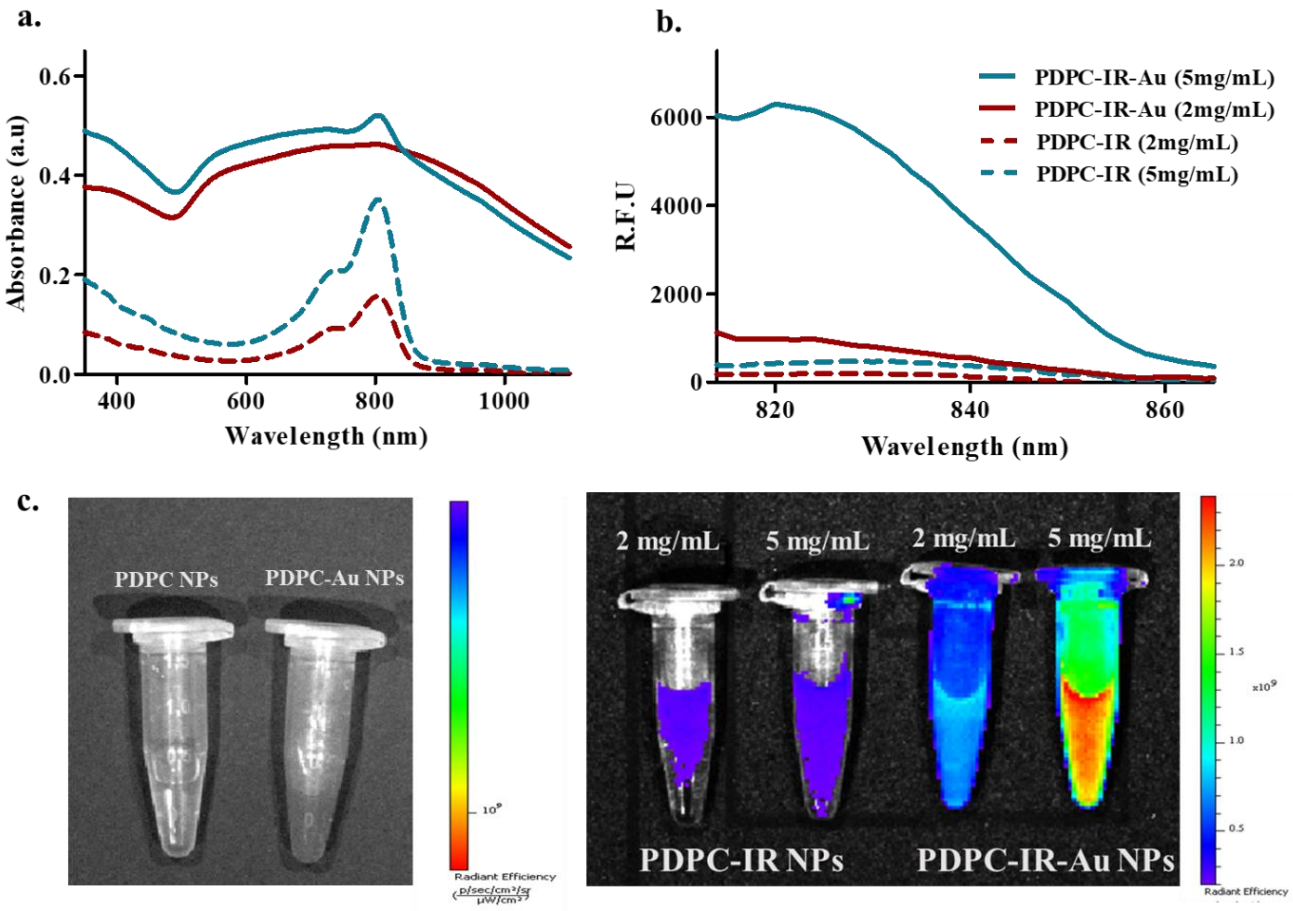

Figure S10: *Spectral characterization of PDPC-IR-Au NPs. a) UV-visible absorbance spectra, b) fluorescence spectra and c) IVIS phantom imaging at different concentrations (of PDPC-IR NPs) before and after coating with gold.*

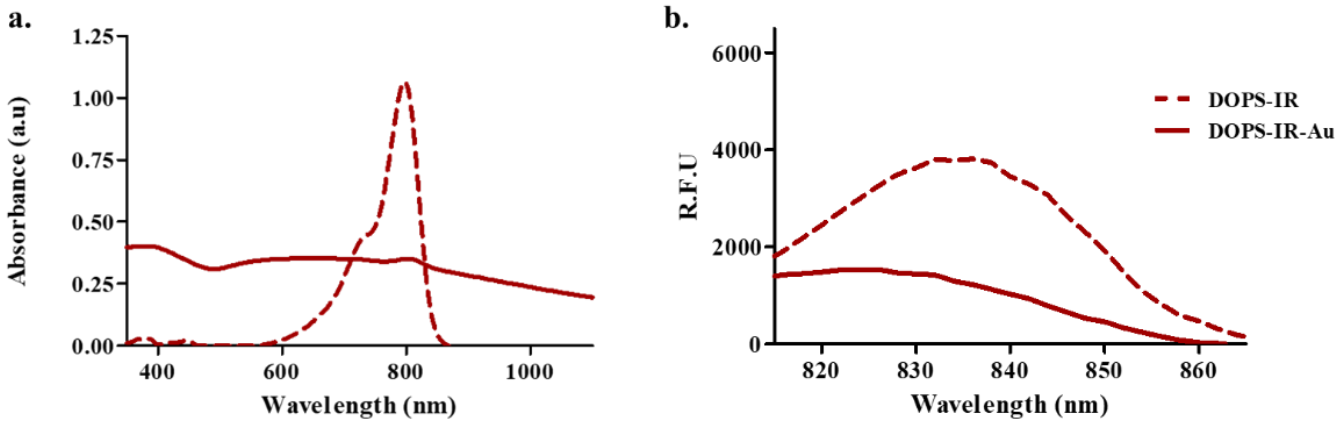

Figure S11: *Spectral characterization of Liposomes loaded with IR780 (DOPS-IR) and coated with gold (DOPS-IR-Au). a) UV-visible absorbance spectra, b) fluorescence spectra before and after coating with gold.*

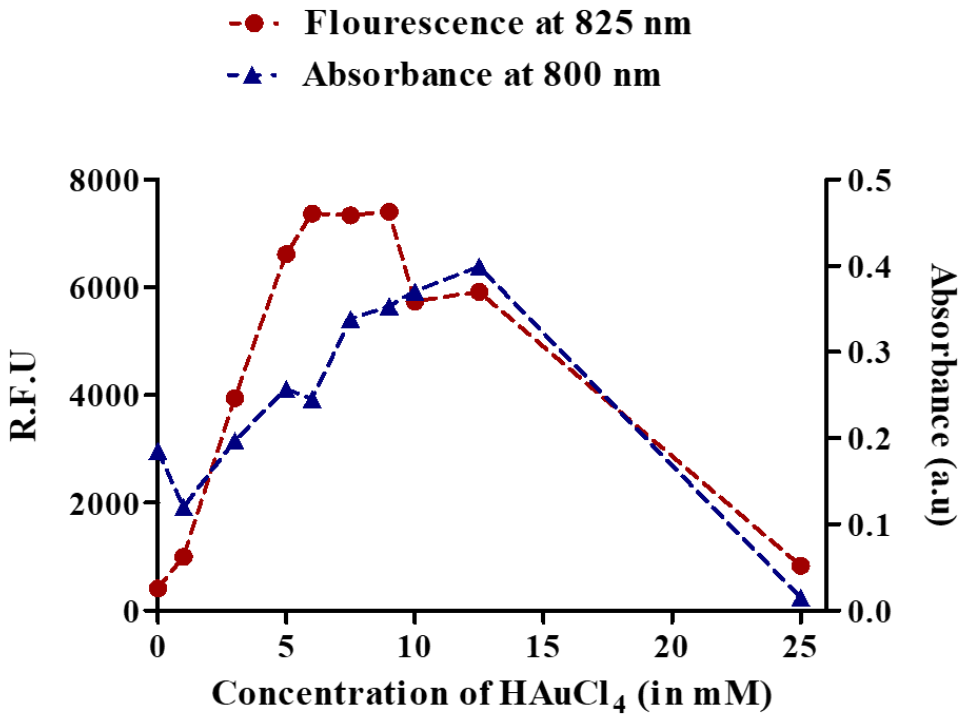

Figure S12: *Changes in the spectral intensities (fluorescence and absorbance) of PDPC-IR-Au NPs with varying concentrations of* $HAuCl_4$.

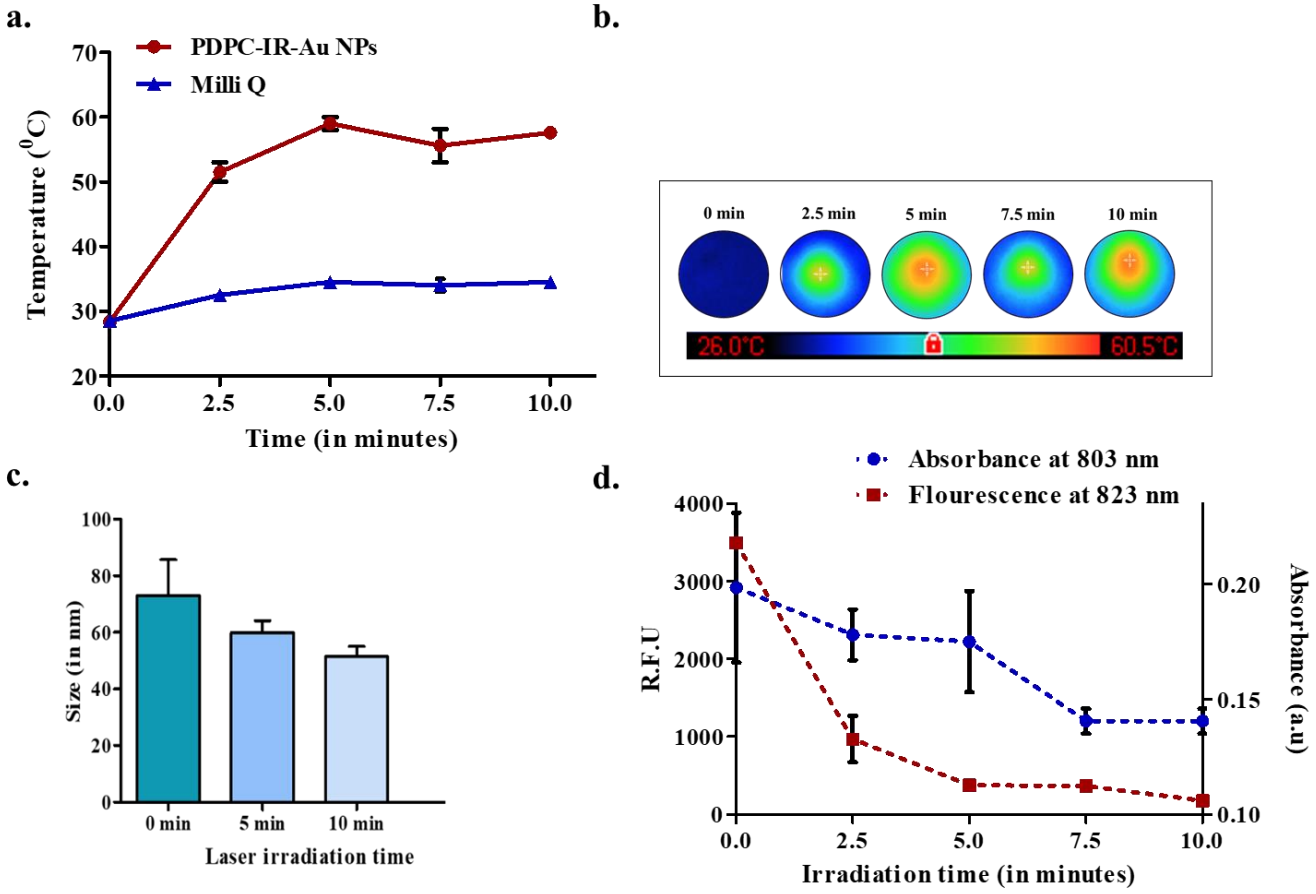

Figure S13: *Photothermal efficacy and its effect on particle size and spectral intensities of PDPC-IR-Au NPs. a) Photothermal efficacy of PDPC-IR-Au NPs, b) Thermal images of PDPC-IR-Au NPs denoting the temperature increment, c) size, d) absorbance and fluorescence intensities of PDPC-IR-Au NPs with laser irradiation time.*

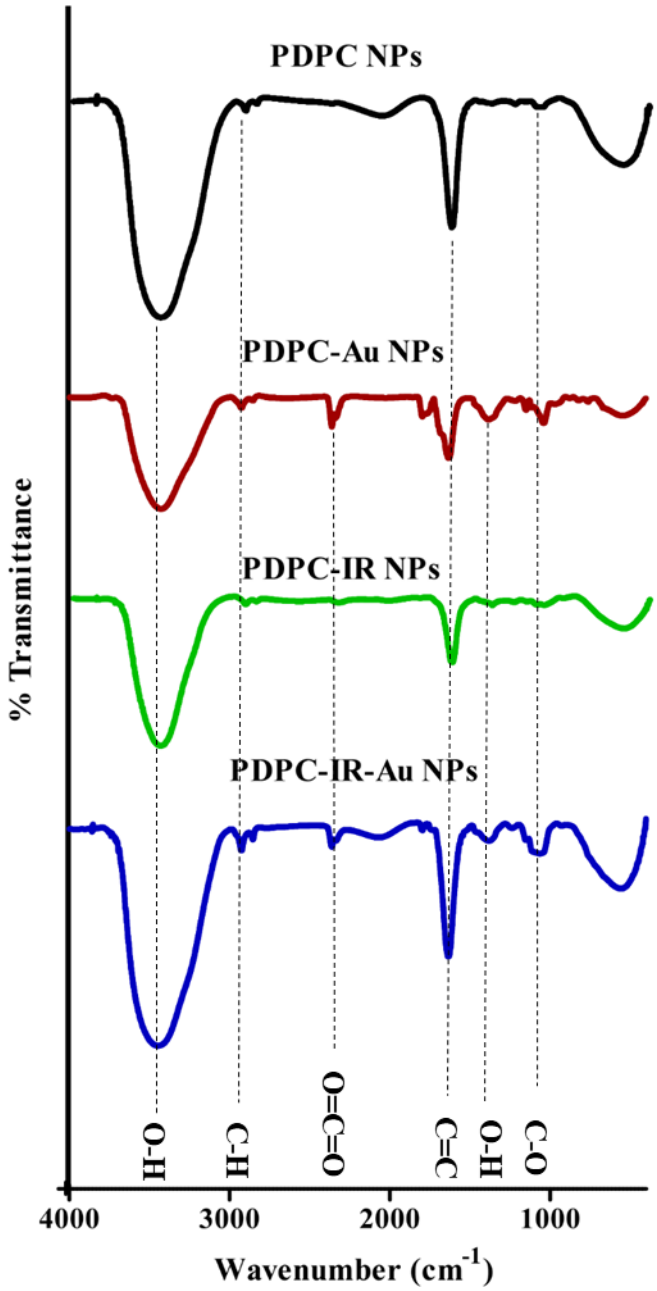

Figure S14: *FTIR spectra of nanoparticles.*

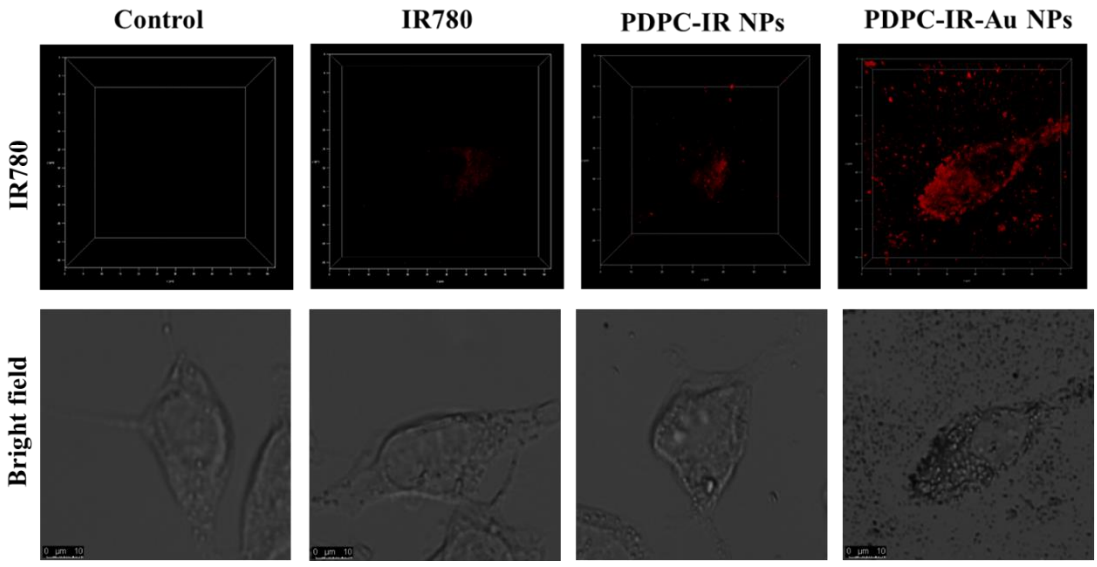

Figure S15: *Confocal microscopy of MCF-7 cells treated with IR780 dye (free), IR780 loaded PDPC (PDPC-IR NPs), IR780 loaded PDPC NPs coated with gold (PDPC-IR-Au NPs) and incubated for 6 hours followed by formaldehyde fixing (*Scale bar corresponds to 10 µm)*

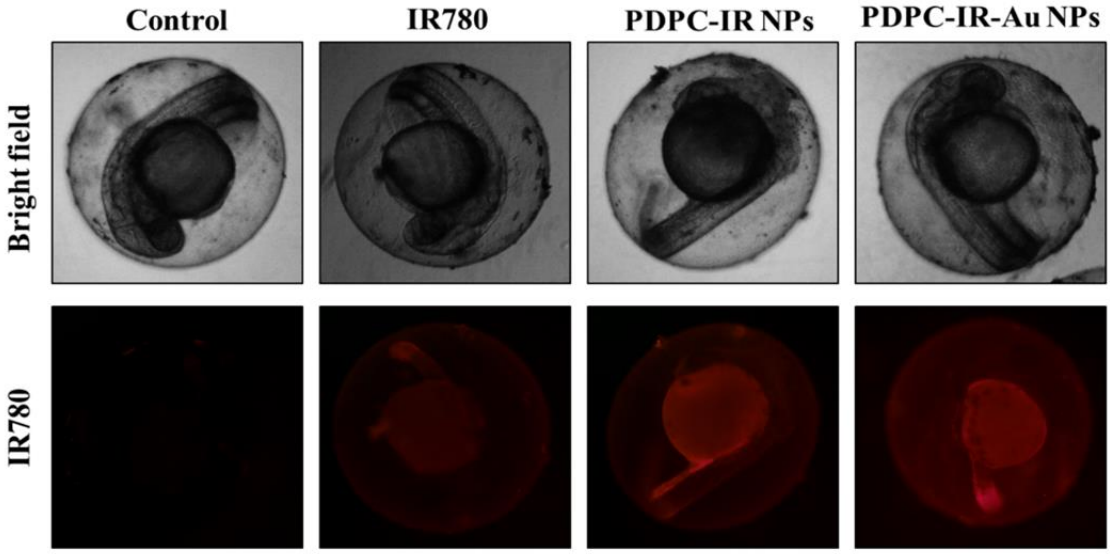

Figure S16: *Zebrafish embryo imaging. Fluorescence microscopy of zebrafish embryos treated with IR780 dye (free), IR780 loaded PDPC (PDPC-IR NPs), IR780 loaded PDPC NPs coated with gold (PDPC-IR-Au NPs) for 48 hours (*Images were captured at 4x).*

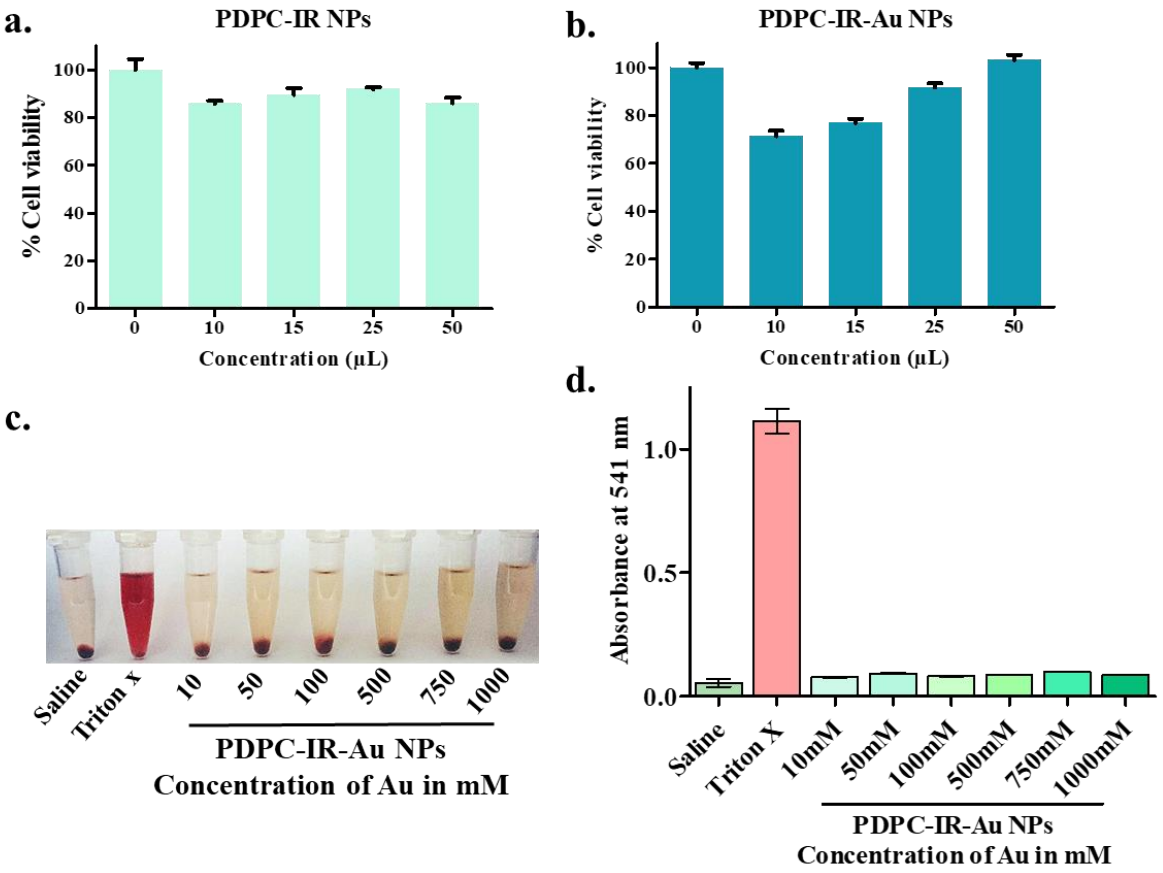

Figure S17: *Biocompatibility and hemolysis of PDPC-IR-Au NPs. Biocompatibility of a) PDPC-IR NPs and b) PDPC-IR-Au NPs in L929 cells, c) Qualitative and d) quantitative representation of hemocompatibility of PDPC-IR-Au NPs over a range of concentrations as compared to Triton x (positive control) and saline (negative control).*

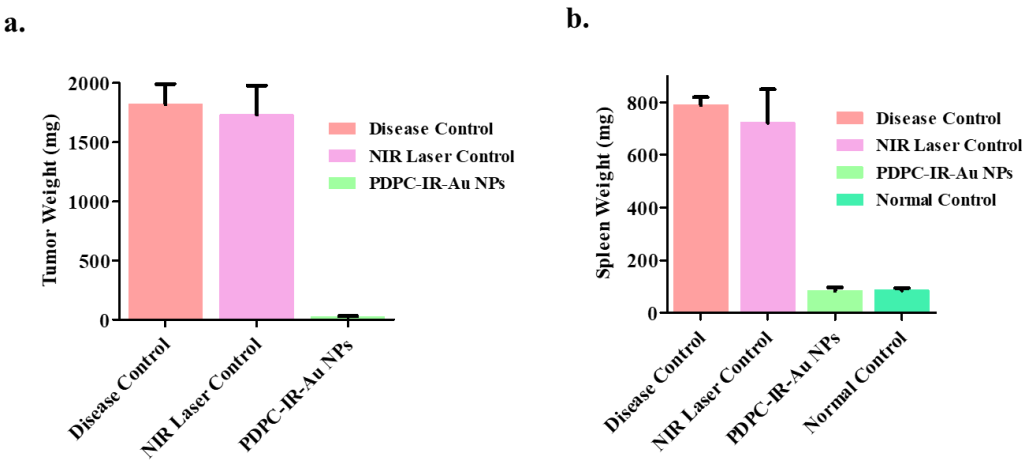

Figure S18: *In-vivo efficacy of PDPC-IR-Au NPs. Weights of a) Tumor and b) spleen collected post-treatment from different groups and their comparison to healthy control.*

Materials and methods

1. Materials

The lipid 1,2-Dioleoyl-sn-glycero-3-phosphoserine, sodium salt (DOPS-Na) was obtained as a generous gift from Lipoid, Germany. Poly ethylene glycol (Mw: 6000), Calcium Chloride anhydrous ($CaCl_2$), Sodium Chloride, Bovine Serum Albumin (pH: 6-7), Sodium hydroxide, Ascorbic acid, MTT (3-(4,5-Dimethylthiazol-2-yl)-2,5-Diphenyltetrazolium Bromide) were procured from SRL Chemicals, India. Polyvinylpyrrolidone (PVP, K-15) was obtained from Merck, Millipore. IR-780 iodide, Hydrogen Tetrachloroaurate(III)/Chloroauric acid ($HAuCl_4.3H_2O$), Fluorescein Diacetate (FDA), 4,6-Diamidine-2-phenylindole dihydrochloride (DAPI), 2,7-dichlorodihydrofluorescein diacetate (DCFH-DA), Propidium Iodide (PI), were purchased from Sigma (St. Louis, MO, USA). Solvents: Methanol, Chloroform, and Dimethyl sulfoxide (DMSO) were procured from SRL chemicals, India. Phosphate buffer pH 7.0, Trypsin-Ethylenediaminetetra aceticacid (EDTA), Dulbecco's Modified Eagle Medium (DMEM), Roswell Park Memorial Institute Medium (RPMI), and Calf Serum (US origin), were purchased from Hi-media Chemicals, (Mumbai, India). All the chemicals were used as received without any further purification.

2. Characterization

The absorption spectra were recorded by a UV-Visible spectrophotometer (UV-1800, Shimadzu, Japan). The fluorescence measurements were recorded by an Enspire multimode plate reader (Perkin Elmer, USA) and Fluorescence spectrophotometer (RF 6000, Shimadzu, Japan). The nanoparticles were imaged under white light and a UV lamp (365 nm) (Analytik Jena, CA, USA). A particle size analyzer measured the hydrodynamic diameter, polydispersity index (PDI) and Zeta Potential (Nicomp Nano Z3000 ZLS, USA). The shape, size and elemental analysis of the nanoparticles were characterized by Field Emission Scanning electron microscopy (FESEM, Carl Zeiss atomic microscope, Supra-40, Germany), JEOL, Transmission Electron Microscopy (TEM) (JEOL, JEM 2100, JEM-2100F, USA) and high-resolution TEM (HR-TEM) (JEOL, Japan). The cellular imaging was performed using a fluorescent microscope (Olympus, CKX-53, USA) and a confocal scanning laser microscope (CSLM, Leica TCS SP8, Germany). The thermal images were captured using FLIR thermal camera (Chauvin Arnoux, CA, 1950 IR camera). 808nm NIR laser (808 nm, 650 mW, Shanghai Inter-Diff Optoelectronics Technology Ltd, Shanghai, China) was used for all the Photothermal experiments. The phantom imaging was performed by the In-vivo Imaging System (IVIS) Lumina fluorescence imaging system (Perkin Elmer, USA).

3. Cell lines & maintenance

Human breast carcinoma (MCF-7) and Mice fibroblast (L929) cell lines were obtained from the National Centre for Cell Sciences (NCCS), Pune, India. Murine breast carcinoma (4T1) cell lines were obtained from AddexBio (C0006004), San Diego. The cell lines were cultured in

DMEM/RPMI medium supplemented with 10% (v/v) Fetal bovine serum (FBS), 1% L-Glutamine, and 100 U/ml penicillin/streptomycin and were maintained at 37 °C in a humidified atmosphere, containing 5% CO_2 under sterile conditions.[1]

4. Zebrafish Husbandry

Zebrafish (Danio rerio) was obtained as a generous gift from CSIR-Centre for Cellular and Molecular Biology (CCMB), Hyderabad, India. Zebrafish were raised and maintained in a closed flow-through culture system at 28 ± 0.5°C in a 14:10 h light−dark cycle. The zebrafish were fed twice a day. In the following light cycle, embryos were collected 2 h postfertilization and washed several times with standard E3 culture media and healthy embryos at the blastula stage were selected for imaging.[2]

5. Synthesis of Lipo-Polymeric hybrid system (PDPC NPs)

The lipo-polymeric hybrid nanosystem was synthesized using modified hydrogel isolation technique.[3, 4] Briefly, liposomes of DOPS-Na with or without drug loading were prepared by thin-film hydration technique.[1, 5, 6] The liposome suspension (10 mg/mL) was added dropwise to the PEG solution (1.98 gms) in water under stirring. The PEG solution with the liposomes was injected into the second hydrogel phase, i.e., PVP (0.52 gms) solution, under constant stirring at room temperature. Calcium chloride (100 mM) was added to the above reaction mixture dropwise, and the solution turned cloudy, indicating the formation of nanoparticles. The mixture was stirred at room temperature for another one hour. After the completion of the reaction, the nanoparticles were recovered by washing the reaction mixture twice with buffer solution (1 mM $CaCl_2$, 150 mM NaCl) followed by centrifugation at 15000 rpm for 60 minutes. The pellet was collected, re-dispersed in buffer solution, subjected to sonication for 10 minutes and stored for future use at 4^oC.

6. PDPC NPs as nanocarriers: Encapsulation of hydrophilic & hydrophobic moieties and their cellular uptake.

6.1 Hydrophilic gold nanoclusters: Albumin gold nanoclusters (GNCs)

Albumin gold nanoclusters (GNCs) were used to show the hydrophilic encapsulation efficacy of PDPC NPs. Albumin gold nanoclusters were synthesized by well-established protocols reported in literature.[7-9] Albumin gold clusters were added into liposomes during the hydration process of liposome formation (L-GNC). The liposomes were added to the PEG solution, and the further synthesis process of PDPC NPs was followed, as mentioned above. The absorbance and fluorescence spectra were recorded. Mean diameter and surface charge were evaluated. Size and morphology were understood using FESEM and TEM imaging. The presence of gold in PDPC-GNCs was confirmed using dark-field imaging and elemental analysis. To demonstrate the

encapsulation efficacy of PDPC NPs over Liposomes, L-GNCs and PDPC-GNCs NPs were centrifuged at 15000 rpm for 30 minutes. The fluorescence under a UV lamp was also recorded, the pellet was re-dispersed, and the fluorescence intensity was measured.

The cellular uptake of PDPC-GNCs was evaluated in MCF-7 cells. The cells were seeded in a 6 well plate at a density of $1x10^5$ cells/well. After 24 hours, PDPC NPs loaded with GNCs, and free GNCs at the same concentration were diluted in fresh media and added to the cells. Free GNCs were also treated at the same concentration to understand the increase in uptake with nanoformulation. Cells without any treatment were considered controls. The cells treated with PDPC-GNCs were harvested at regular time intervals of 6, 12 and 24 hours, while cells treated with only GNCs were only collected after 24 hours of treatment. The cells were washed and processed for FACS analysis.[1]

6.2 Hydrophobic IR780 dye

IR780, a NIR dye was used to demonstrate the hydrophobic encapsulation of PDPC NPs.[10] IR780 was dissolved in methanol and added to the lipid (in the ratio of 0.5:10) during the thin film process, and the thin-film hydration technique was used to synthesize IR780 loaded liposomes (DOPS-IR780). The liposomes were added to the PEG solution, and the synthesis protocol for PDPC NPs was followed, as mentioned above. The IR780 loaded PDPC NPs were green in colour and were stored at 4^{o}C following washing and sonication. The PDPC-IR NPs were subjected to absorbance and fluorescence spectroscopy to confirm the encapsulation of IR780. The size and morphology of PDPC-IR NPs were understood by TEM imaging. The cellular uptake was studied as follows. MCF-7 cells were seeded on a coverslip in a 6 well plate at a $1x10^5$ cells/well density. After 24 hours, PDPC NPs loaded with IR780, i.e. PDPC-IR NPs and free IR780, were diluted in fresh media and added to the cells, with the concentration of IR780 constant. Cells without any treatment were considered controls. Following 6 hours of incubation, the cells were washed thrice with PBS and fixed using 4% formaldehyde. The cells were imaged using confocal scanning laser microscopy with the emission channel in 600-800 nm and excited by 633 nm laser.[1, 10]

7. PDPC NPs for Photothermal therapy: PDPC-Au NPs.

7.1 Synthesis and characterization of PDPC-Au NPs:

PDPC-Au NPs were prepared using *in-situ* chemical reduction using ascorbic acid as a reducing agent[5, 11, 12]. PDPC NPs (100 µL, 2 mg/mL) were mixed with 100 µL of $HAuCl_4.3H_2O$ (5 mM). Ascorbic acid (200 µL, 10 mM) was added to the reaction mixture, and a change in colour from yellow to blue was observed and captured, which indicated the formation of PDPC-Au NPs. The change in colour at different reaction times was noted, and the sample was collected at these regular intervals. The samples were characterized for their absorbance and morphology to understand their growth process. The effect of the concentration of $HAuCl_4.3H_2O$ on the

absorbance, sizes and shape of PDPC-Au NPs was evaluated to optimize the synthesis protocol of PDPC-Au NPs. The PDPC-Au NPs were characterized to evaluate their NIR absorbance, shape and size using FESEM and TEM. The surface coating of gold was observed using the dark field TEM imaging, and the presence of gold on the surface was confirmed by lattice fringes, SAED patterns and elemental analysis. The differences in absorption spectra and morphology of PDPC NPs was compared to liposomes (DOPS-Na) coated with gold using the same concentrations of $HAuCl_4.3H_2O$ and ascorbic acid.

7.2 Stability of PDPC-Au NPs:

The stability of PDPC-Au NPs and Lipos-Au NPs (DOPS-Na liposomes coated with gold) was evaluated by mixing the nanoformulations with 250 µL of fetal bovine serum, a vital cell growth nutrient used in cell culture media and left undisturbed for 36 hours. The images were captured at 0 and 36 hours and were observed for aggregations or agglomerations due to the protein and particle interactions.[2]

7.3 Photothermal efficacy and calculation of PTT conversion efficiency:

The photothermal efficacy was evaluated as follows. The PDPC-Au NPs (100 µL) and Milli-Q water were subjected to 808 nm NIR laser irradiation for 2.5, 5.0, 7.5 and 10 min. The initial and final temperatures were recorded. The thermal images corresponding to the rise in temperature were recorded using a thermal imaging camera. The photothermal conversion efficacy of the PDPC-Au NPs was determined as reported in literature.[13-15] Briefly, 3 mL of PDPC-Au NPs dispersed in Milli-Q water was taken in a quartz cuvette and subjected to NIR laser irradiation (808 nm, 650 mW) with continuous measurement of temperature. After the temperature reached a steady state, the NIR laser was turned off, and the dispersion was allowed to cool to room temperature. The temperature decrease was measured throughout the process. Similarly, the heating and cooling curve of water was also determined, and the curves were plotted. The Photothermal conversion efficacy was calculated using the formula

$$\eta = \frac{hS(T_{Max} - T_{Surr}) - Q_{Dis}}{I(1 - 10^{-A808})}$$

Where η is the photothermal conversion efficiency of PDPC-Au nanoparticles, h and S denote the sample cell's heat transfer coefficient and surface area, respectively. T_{max} is the maximum temperature attained by PDPC-Au NPs with laser irradiation (808 nm, 650 mW), and T_{surr} is the surrounding ambient room temperature. Q_{Dis} denotes the baseline energy of the heat generated from water and the sample cell. I is the laser power (650 mW, 3 Wcm−2) and A808, the absorbance of PDPC-Au NPs at 808 nm.

7.4 Degradation and disintegration of PDPC-Au NPs.

The PDPC-Au NPs irradiated for 2.5, 5 and 10 minutes were collected and analyzed for their absorbance and size (using a Particle size analyzer for n = 3). PDPC-Au NPs were irradiated for 10 minutes using an 808 nm NIR laser, and the sample was characterized by TEM to understand the disintegration with laser irradiation.[15]

7.5 In-vitro studies of PDPC-Au NPs.

7.5.1 Biocompatibility

L929 cells (Mouse fibroblasts) were seeded in a 96 well plate at a density of $1x10^4$ cells/well 24 hours before the experiment. PDPC NPs and PDPC-Au NPs were diluted in cell culture media, amounting to different concentrations. The nanoparticles were incubated with cells for 24 hours, and cell viability assay was performed at the end of 24 hours using MTT assay, and viabilities were calculated.[16]

7.5.2 Photothermal mediated cytotoxicity & Live/Dead assay

MCF-7 cells were seeded in a 96-well plate at a $1x10^4$ cells/well density. After 24 hours, PDPC-Au NPs (25 and 50 µL) were added to the wells and subjected to NIR irradiation for 5, 7.5, and 10 minutes. After 24 hours, using a standard protocol, the methyl thiazolyl tetrazolium (MTT) assay was performed to determine cell viability. Cells without any treatment and cells treated only with PDPC-Au NPs or NIR laser were considered controls. Groups treated with only particles treatment or NIR light were considered experimental controls. A live/dead assay was performed in MCF-7 cells using FDA/PI staining for qualitative assessment of photothermal cytotoxicity. MCF-7 cells were treated with PDPC-Au NPs in DMEM media, followed by NIR light irradiation for 5 min. Cells without any treatment (Control group), cells incubated with PDPC-Au NPs only (PDPC NPs), and cells irradiated by NIR laser without co-incubation of NPs (Control + laser group) were considered controls. Twenty-four hours post-treatment, cells were stained with FDA and PI dyes to stain live and dead cells, respectively. The cells were washed and subjected to fluorescent microscopy to observe and record live and dead cells in each group fluorescing in green and red, respectively.[1]

7.5.3 Photothermal mediated Intracellular ROS evaluation: DCFH-DA assay

Intracellular ROS levels were measured using a fluorescent dye, dichlorodihydrofluorescin diacetate (DCFH-DA), which could be rapidly oxidized into the highly fluorescent 2',7' dichloro-fluorescein (DCF) in the presence of intracellular ROS. To detect the intracellular ROS, MCF-7 cells were treated with PDPC-Au NPs, followed by NIR laser irradiation for 5 minutes. Cells

without any treatment, with only NPs or NIR laser irradiation, were considered controls. After 5 hours, the cells were stained with DCFH-DA (25 μM) and incubated for around 45 minutes. The sample was then observed under fluorescence microscopy (green fluorescence indicating the presence of ROS), and the fluorescence intensity was measured under excitation at 488 nm and emission at 525 nm using a fluorescence microplate reader. ROS levels were compared with the viabilities and expressed as fold-change over control.[1, 17]

7.5.4 Photothermal mediated DNA damage

The photothermal mediated DNA damage was evaluated in MCF-7 cells using ϒH2A.X assay[13, 18] and Comet assay.[19, 20]

7.5.4.1 ϒH2A.X assay

For ϒH2A.X assay, $5x10^5$ cells were plated on pre-treated coverslips 48 hours before performing immunofluorescence. The next day, cells were washed thrice with PBS and incubated with PDPC-Au NPs for 6 hours. The respective groups were irradiated with NIR laser (808 nm, 650 mW) for 5 minutes. 1-hour post-treatment, cells were fixed with 4% paraformaldehyde for 10 minutes at 37°C. The cells were then permeabilized in 4% paraformaldehyde with 0.2% Triton X-100 (Sigma Aldrich, USA) for 10 minutes. Cells were again washed thrice with PBS and blocked with 2% BSA in PBS for 30 minutes at room temperature. Cells were incubated with the α-phospho-H2A.X primary antibody in a humidified chamber overnight at 4°C. Cells were washed 3 times with PBS the next day and incubated with the ϒH2A.X respective dye labelled Dylight 633 secondary antibody. Nuclei were counterstained with DAPI (5 μg/ml). Images were captured using the Zeiss LSM 510 Meta Confocal Microscope (Carl Zeiss, Germany).[18]

7.5.4.2 Comet assay

The DNA fragmentation was assessed by comet assay. MCF-7 cells were seeded into 96-well plates 24 hours before the experiment. Cells were treated with PDPC-Au NPs and subjected to NIR light irradiation for 5 minutes. MCF-7 cells treated only with PDPC-Au NPs or NIR laser were used as experimental controls. Untreated cells were considered a negative control. After 24 h incubation, the cells were washed with PBS, scraped, centrifuged, and suspended in 100 μL PBS. For slide preparation, the frosted microscope slides were dipped in regular molten agarose and dried in air at 50 ^{0}C. Then, the cell containing a layer of agarose (1.0%) was added and dried two times. The prepared slides were put in a lysis solution containing 2.5 M NaCl, 100 mM EDTA, 1% N-lauroylsarcosine and 10 mM Trizma at pH 10.0 for 1 h. Furthermore, 1% Triton X-100 was added just before usage. The slides were incubated in an alkaline (pH > 13) electrophoresis buffer for 20 min to obtain single-stranded DNA (ss-DNA). The alkaline solution contained 1 mM EDTA and 300 mM NaOH. Then, the obtained ss-DNA gel was electrophoresed at 1.0 V cm^{-1} for 20 min

under the same alkaline conditions to produce comets. After the electrophoresis, the alkali in the gel was removed by washing the slides using Trizma at pH 7.5. The DNA-specific dye, ethidium bromide, a red fluorescent dye, was used for comet observation under fluorescent microscopy.[21, 22]

8. PDPC NPs as Plasmon resonant fluorescent nanosystems for imaging and therapeutic applications.

8.1 Synthesis and characterization of PDPC-IR-Au NPs: IR780 loaded PDPC NPs coated with Au.

The PDPC-IR NPs are synthesized as mentioned in section 1.2. PDPC-IR-Au NPs were prepared using the same protocol as described for PDPC-Au NPs. Briefly, PDPC-IR NPs (100 µL, 2 mg/mL) were mixed with 100 µL of $HAuCl_4.3H_2O$ (5 mM). Ascorbic acid (200 µL, 10 mM) was added to the reaction mixture, and a change in colour from yellow to greenish-blue was observed, indicating the formation of PDPC-IR-Au NPs. The PDPC-IR-Au NPs are characterized for their absorbance and fluorescence. For comparison, the DOPS-Na Liposomes loaded with IR780, i.e., DOPS-IR, were also subjected to surface coating with gold and the changes in the spectral intensities were noted. The concentrations of ascorbic acid and $HAuCl_4.3H_2O$ were the same. The concentration of IR780 in both PDPC-IR NPs and DOPS-IR NPs was maintained the same. The changes in absorbance and fluorescence of PDPC-IR-Au NPs were also measured by increasing the concentration of PDPC-IR NPs from 2 mg/mL to 5 mg/mL. The samples PDPC NPs, PDPC-Au NPs, PDPC-IR NPs (2 mg/mL and 5 mg/mL) and corresponding PDPC-IR-Au NPs were subjected to *in-vivo* phantom imaging to observe the enhanced fluorescence with surface coating. To understand the effect of the concentration of $HAuCl_4.3H_2O$ on the surface plasmon-enhanced fluorescence of PDPC-IR-Au NPs, the absorbance and fluorescence at the peak maxima of PDPC-IR-Au NPs were measured with varying concentrations. The PDPC-IR-Au NPs were further analyzed by TEM imaging to understand the size and morphology.

8.2 PDPC-IR-Au NPs for imaging of cancer cells and zebrafish embryos.

8.2.1 MCF-7 cells:

The cellular imaging was performed in MCF-7 cells following the below protocol. MCF-7 cells were seeded on a coverslip in a 6 well plate at a $1x10^5$ cells/well density. After 24 hours, PDPC NPs loaded with IR780, i.e. PDPC-IR NPs, free IR780 and PDPC-IR-Au NPs, were diluted in fresh media and added to the cells concentration of IR780 maintained the same in all the three groups amounting to 2 µg per well. Cells without any treatment were considered controls. Following 6 hours of incubation, the cells were washed thrice with PBS and fixed using 4% formaldehyde. The cells were imaged using confocal scanning laser microscopy with the emission

channel range 600-800 nm and excited by 633 nm laser.[1, 10] A 3D imaging view was recorded in confocal microscopy by magnifying a single cell.

8.2.2 Zebrafish embryos:

Zebrafish embryos were collected at 2 h post-fertilization (hpf) and washed thrice using a standard E3 culture medium. The embryos were distributed 10 per well in 2 mL of media in a six-well plate. The embryos were subjected to PDPC-IR-Au NPs, PDPC-IR NPs, and free IR780 with the concentration of IR780 constant in all the treatment groups (0.5 µg per well). The untreated embryos were considered controls. Following incubation for 48 hours, the embryos were washed and subjected to fluorescent microscopy imaging (Olympus CKX-53, USA).[2]

8.3 *In-vitro* Experiments: PDPC-IR-Au NPs.

8.3.1 Biocompatibility

L929 cells (Mouse fibroblasts) were seeded in a 96 well plate at a density of $1x10^4$ cells/well 24 hours prior to the experiment. PDPC-IR and PDPC-IR-Au NPs were diluted in cell culture media, amounting to different concentrations. The nanoparticles were incubated with cells for 24 hours, and a cell viability assay was performed using MTT assay.[1, 23]

8.3.2 Photothermal mediated cytotoxicity

The photothermal mediated cytotoxicity analysis was performed in both MCF-7 and 4T1 cells. The cells were seeded in a 96-well plate at a density of $1x10^4$ cells/well. After 24 hours, PDPC-IR-Au NPs diluted in cell culture media were added to the wells and subjected to NIR irradiation for 5 minutes. After 24 hours, using a standard protocol, the methyl thiazolyl tetrazolium (MTT) assay was performed to determine cell viability. Cells without any treatment and cells treated with PDPC-IR-Au NPs/NIR laser were considered controls.[1]

8.4 Hemolysis experiment

Hemolysis was evaluated to determine the hemocompatibility of the nanosystem[13, 24]. Briefly, the blood sample was obtained and centrifuged at 3000 rpm for 15 minutes. The plasma was removed, and RBCs were washed with standard saline solution three times until the supernatant was clear. The RBCs were counted following their dispersion in normal saline. Briefly, 1.5×10^7 RBCs were suspended in 950 µL of saline and incubated with 50 µL of saline (negative control), Triton × 100 (positive control), and different concentrations of PDPC-IR-Au NPs at 37 °C for 1 h and centrifuged at 3000 rpm for 10 min. The absorbance at 540 nm was used to determine the degree of hemolysis in the supernatant.

8.5 *In-vivo* Experiments.

8.5.1 Development of 4T1 breast cancer model in mice

The *in-vivo* experiments were conducted according to CPCSEA guidelines and the Institutional Animal Ethics Committee of G. Pulla Reddy College of Pharmacy, Hyderabad (GPRCP/IAEC-02/29/12/2021/PCL-14). The experiments were conducted in female Balb/C mice (4-6 weeks) procured from Hylasco Bio-Technology Pvt. Ltd, Hyderabad. The breast cancer model was established by injecting 1×10^6 4T1 cells/animal subcutaneously to the dorsal flank region of female Balb/C mice. When the tumour reached ~150-200 mm^3, the animals were randomly grouped into three groups (Disease control, NIR Laser control, PDPC-IR-Au NPs groups, respectively).[1]

8.5.2 Photothermal imaging and therapy *in-vivo.*

The photothermal transduction efficiency of the PDPC-IR-Au NPs was evaluated as follows: the nanoparticles were injected intratumorally, followed by 808 nm NIR laser irradiation for 2 min in 3 directions, accounting for a total of 6 minutes of irradiation. The increment in temperature was measured at regular intervals (0, 2, 4, and 6 minutes), and subsequent thermal images were captured using a thermal imaging camera (Chauvin Arnoux, CA,1950 IR camera, USA). The *in-vivo* antitumor efficiency of the PDPC-IR-Au NPs (1mg of Au concentration) was evaluated by three treatment cycles at 4 days intervals. The mice were monitored continuously, and a Vernier calliper was used to measure the tumour growth by measuring the tumour volume (length, width, and height). At the end of the study, the mice were sacrificed, and the organs and tumours were isolated for further analysis. The tumours and spleen collected from the animals in the different groups were weighed, and the graphs were plotted. A survival curve has been plotted using the survival data of animals in each group. The spleens collected from mice from different treatment groups were imaged and compared to healthy control mice to understand the therapeutic efficacy of the PDPC-IR-Au NPs.[1, 25, 26]

8.5.3 Statistical analysis

Mean ± SEM values were used for the expression of data. Statistical analyses of data were performed using the Student's t-test or two-way ANOVA. Values of $p < 0.05$ were considered statistically significant. (The statistical significance was denoted as follows: for $p > 0.05$: non-significant (ns), for $p < 0.05$: *, for $p < 0.001$: ***)

References:

1. T. Appidi, D. B. Pemmaraju, R. A. Khan, S. B. Alvi, R. Srivastava, M. Pal, N. Khan and A. K. Rengan, *Nanoscale*, 2020, **12**, 2028-2039.
2. A. Thomas, T. Appidi, A. B. Jogdand, S. Ghar, K. Subramaniyam, G. Prabusankar, J. R. Mohanty and A. K. Rengan, *ACS Applied Polymer Materials*, 2020, **2**, 1388-1397.
3. L. Zarif, J. R. Graybill, D. Perlin and R. J. Mannino, *Journal of liposome research*, 2000, **10**, 523-538.
4. T. Jin, L. Zarif and R. Mannino, *Journal*, 2000.
5. A. K. Rengan, M. Jagtap, A. De, R. Banerjee and R. Srivastava, *Nanoscale*, 2014, **6**, 916-923.
6. S. P. Singh, S. B. Alvi, D. Bharadwaj, A. D. Singh, S. V. Manda, R. Srivastava and A. K. Rengan, *Int. J. Biol. Macromol.*, 2018, **110**, 375-382.
7. X. Le Guével, B. Hötzer, G. Jung and M. Schneider, *Journal of Materials Chemistry*, 2011, **21**, 2974-2981.
8. J. Xie, Y. Zheng and J. Y. Ying, *J. Am. Chem. Soc.*, 2009, **131**, 888-889.
9. M. Shaji, T. Appidi, S. Jain, A. K. Rengan and H. N. Unni, *Microfluidics and Nanofluidics*, 2021, **25**, 1-8.
10. D. Pemmaraju, T. Appidi, G. Minhas, S. P. Singh, N. Khan, M. Pal, R. Srivastava and A. K. Rengan, *Int. J. Biol. Macromol.*, 2018, **110**, 383-391.
11. T. S. Troutman, J. K. Barton and M. Romanowski, *Advanced Materials*, 2008, **20**, 2604-2608.
12. S. B. Alvi, T. Appidi, B. P. Deepak, P. Rajalakshmi, G. Minhas, S. P. Singh, A. Begum, V. Bantal, R. Srivastava and N. Khan, *Biomaterials science*, 2019, **7**, 3866-3875.
13. A. Pradhan, A. Kumari, R. Srivastava and D. Panda, *ACS Applied Bio Materials*, 2019, **2**, 5727-5738.
14. D. S. Chauhan, M. K. Kumawat, R. Prasad, P. K. Reddy, M. Dhanka, S. K. Mishra, R. Bahadur, S. Neekhra, A. De and R. Srivastava, *Colloids and Surfaces B: Biointerfaces*, 2018, **172**, 430-439.
15. D. S. Chauhan, R. Prasad, J. Devrukhkar, K. Selvaraj and R. Srivastava, *Bioconjug. Chem.*, 2017, **29**, 1510-1518.
16. D. B. Pemmaraju, T. Appidi and A. K. Rengan, 2019.
17. L. Wang, J. Shi, R. Liu, Y. Liu, J. Zhang, X. Yu, J. Gao, C. Zhang and Z. Zhang, *Nanoscale*, 2014, **6**, 4642-4651.
18. A. K. Rengan, A. B. Bukhari, A. Pradhan, R. Malhotra, R. Banerjee, R. Srivastava and A. De, *Nano Lett.*, 2015, **15**, 842-848.
19. S. B. Alvi, S. Paradkar, A. Pradhan, R. Srivastava and A. K. Rengan, 2019.
20. S. V. Mudigunda, D. B. Pemmaraju, S. Paradkar, E. R. Puppala, B. Gawali, S. M. Upadhyayula, N. Vegi Gangamodi and A. K. Rengan, *ACS Biomater Sci Eng*, 2022, **8**, 151-160.
21. O. Akhavan, E. Ghaderi and H. Emamy, *Journal of Materials Chemistry*, 2012, **22**, 20626-20633.
22. R. R. Tice, E. Agurell, D. Anderson, B. Burlinson, A. Hartmann, H. Kobayashi, Y. Miyamae, E. Rojas, J. C. Ryu and Y. Sasaki, *Environ. Mol. Mutagen.*, 2000, **35**, 206-221.
23. A. Shanavas, A. K. Rengan, D. Chauhan, L. George, M. Vats, N. Kaur, P. Yadav, P. Mathur, S. Chakraborty and A. Tejaswini, *Int. J. Biol. Macromol.*, 2018, **110**, 392-398.
24. D. S. Chauhan, B. P. K. Reddy, S. K. Mishra, R. Prasad, M. Dhanka, M. Vats, G. Ravichandran, D. Poojari, O. Mhatre and A. De, *Langmuir*, 2019, **35**, 7805-7815.
25. R. PS, S. B. Alvi, N. Begum, B. Veeresh and A. K. Rengan, *Biomacromolecules*, 2021, **22**, 3926-3940.

26. S. Baseeruddin Alvi, R. PS, N. Begum, A. B. Jogdand, B. Veeresh and A. K. Rengan, *ACS Applied Materials & Interfaces*, 2021, **13**, 55862-55878.